ECT
Engineering College of Technology.

Beyond PI Control: Optimal and Observer-Based Control of the Vienna Rectifier

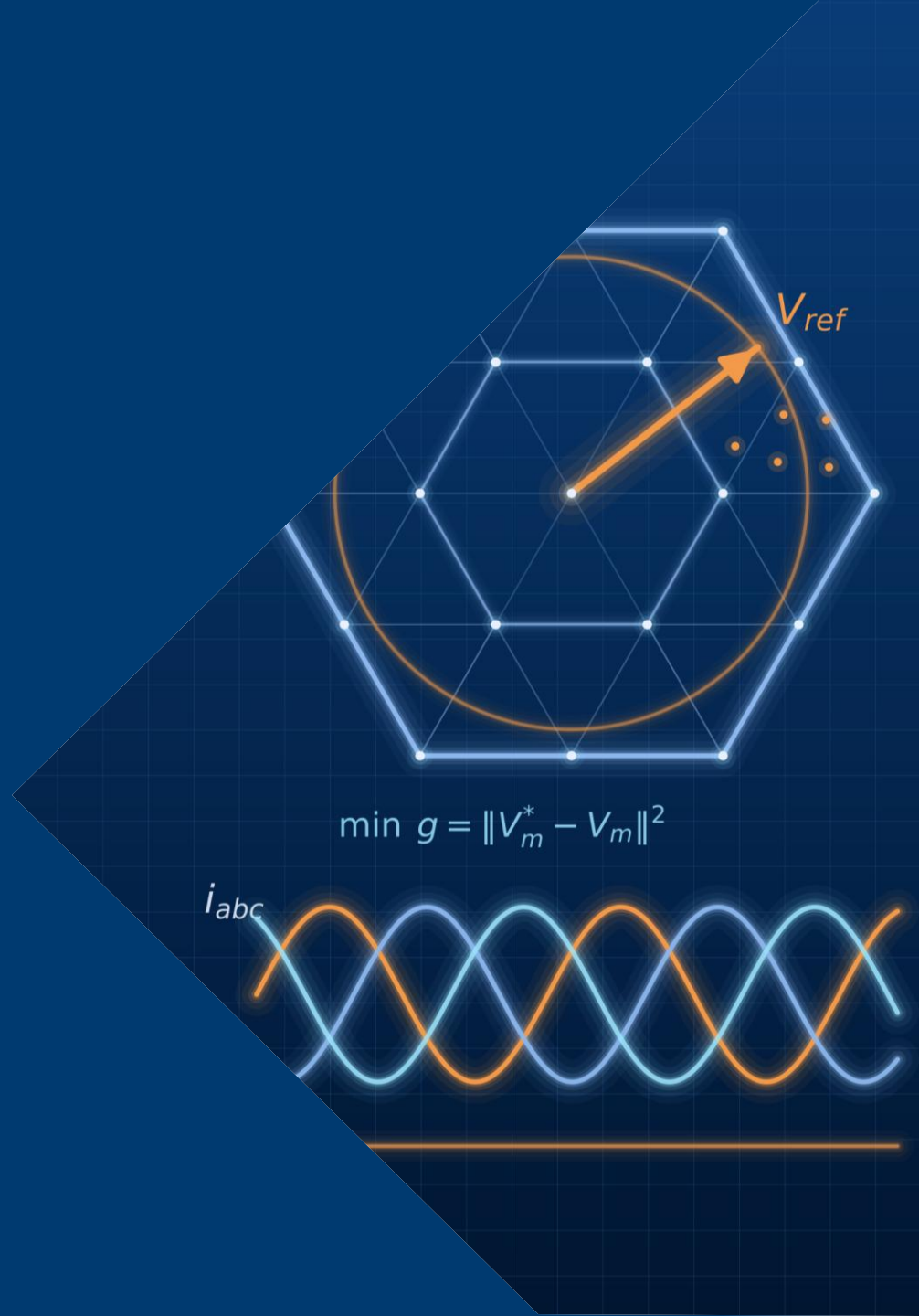

Watch Webinar Recording Here

Dr Tawfique Uzzaman | Lecturer, Power Electronics

UKPRN: 10089771

About ECT

We are dedicated to ensuring that you receive a world-class education and gain skills that you can immediately apply in the workforce.



Engineering Specialists

ECT - affiliated to the well-established Engineering Institute of Technology (EIT) - is an engineering education specialist. ECT delivers bachelor's and master's degrees.



Industry-Driven programmes

Our programmes are designed by industry experts, ensuring you graduate with cutting-edge skills that are valued by employers. Our programme content remains current with rapidly changing technology and industry developments.



UK Recognised Education

ECT is OfS registered, meeting the Office for Students' requirements for course quality, academic standards, student support and student protection.



Lecturers and Instructors

Our teachers are subject specialists with industry experience and the requisite academic qualifications. They bring extensive expertise from across the engineering sector, ensuring students learn from experienced professionals with both academic and real-world knowledge.



Unique Delivery Model

We deliver our programmes via a unique delivery methodology that makes use of live and interactive tutorials, an international pool of expert lecturers, dedicated learning support officers, hands-on workshops and state-of-the-art remote labs connected to real equipment, and simulation software.

UKPRN: 10089771

Introduction – Presenter

Dr. Tawfique Uzzaman



- Lecturer and tutor in power electronics and power systems at EIT
- R&D Engineer in power electronics (industry) and Research Assistant, Edith Cowan University
- PhD in Electrical Engineering, The University of Western Australia (2026): advanced control of three-level Vienna rectifiers
- M.S. Electrical Engineering, Soongsil University, Seoul (2021); former Research Engineer, ADTechnology Co., Seoul
- B.Sc. Electrical and Electronic Engineering, Green University of Bangladesh (2017)
- Research: model predictive control, disturbance observers, sensorless control, grid-connected converters and microgrids

Agenda

	Section	Approx.
1	Why the Vienna rectifier needs better control	10 min
2	What the literature offers	6 min
3	Optimal control I: improved LADRC + FCS-MPC	8 min
4	Optimal control II: LQR + virtual-vector MPC	7 min
5	Observer-based control: removing the current sensors	8 min
6	Comparison and design guidance	6 min



Key terms used today

Term	Meaning
PFC	Power factor correction: shaping the input current to follow the grid voltage
PF	Power factor: 1.0 means all the current does useful work
THD	Total harmonic distortion of the current, % of the 50 Hz component
DC link, NPV	The two output capacitors and the voltage at their midpoint (neutral point)
PI	Proportional-integral controller: the classical feedback loop
PLL	Phase-locked loop: tracks the grid angle

Term	Meaning
FCS-MPC	Finite-control-set model predictive control: try every switch state on a model, apply the best
Virtual vector	An average of two or three real switch states applied within one sample
LQR	Linear quadratic regulator: gains chosen by minimising error plus effort
LADRC, LESO	Linear active disturbance rejection control; its extended state observer estimates disturbances
RLS	Recursive least squares: updates estimates online as data arrives
MP-LESO	The hybrid observer of [3] that estimates the phase currents

Part 1 of 6

Why the Vienna rectifier needs better control

One bidirectional switch per phase, three levels, and a control problem PI alone cannot solve

Why a rectifier needs power factor correction

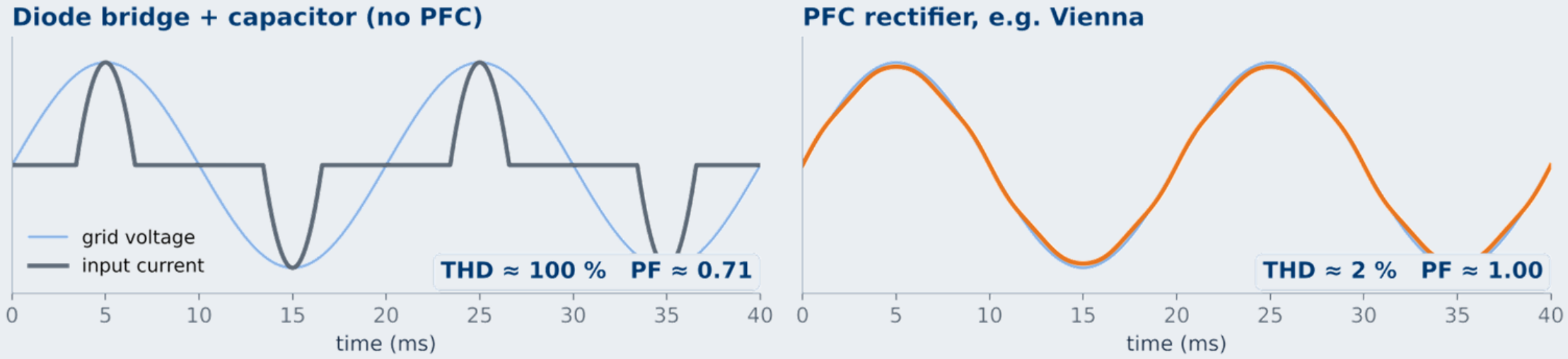

Fig. 1. Illustrative input current without and with power factor correction (computed waveforms).

Power factor (PF)

Share of the current that does useful work; 1.0 = sinusoidal and in phase with the voltage

Harmonic distortion (THD)

Harmonic current as % of the 50 Hz component; standards such as IEEE 519 typically ask for about 5 % or less

PFC rectifier

Switches actively so the current follows the voltage: PF ≈ 1, THD of a few %

The Vienna rectifier: a three-level PFC front end

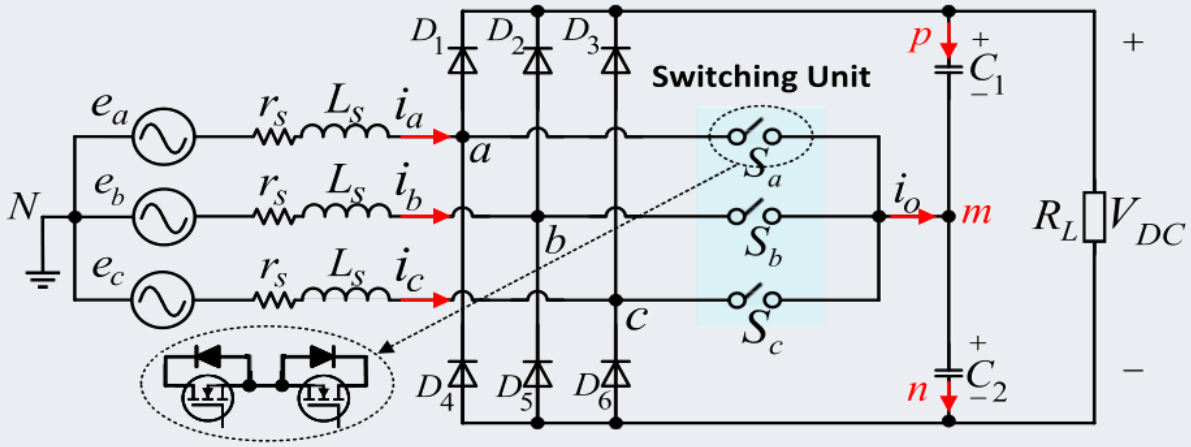

Fig. 2. Three-phase three-level Vienna rectifier: diode bridge plus one bidirectional switch per phase [2].

- **Three-level PFC rectifier** introduced by Kolar and Zach [4]
- **One switch per phase:** no shoot-through, so no dead time
- Each switch blocks only $V_{dc}/2$
- Sinusoidal input current at **unity power factor**
- EV chargers, telecom/data-centre supplies, wind generators [1], [5]

1 pair switch per phase
vs 4 per phase in NPC / T-type

25 states, 19 vectors
three-level space vector set

Unidirectional
boost-type AC/DC only

How one phase of the Vienna rectifier works

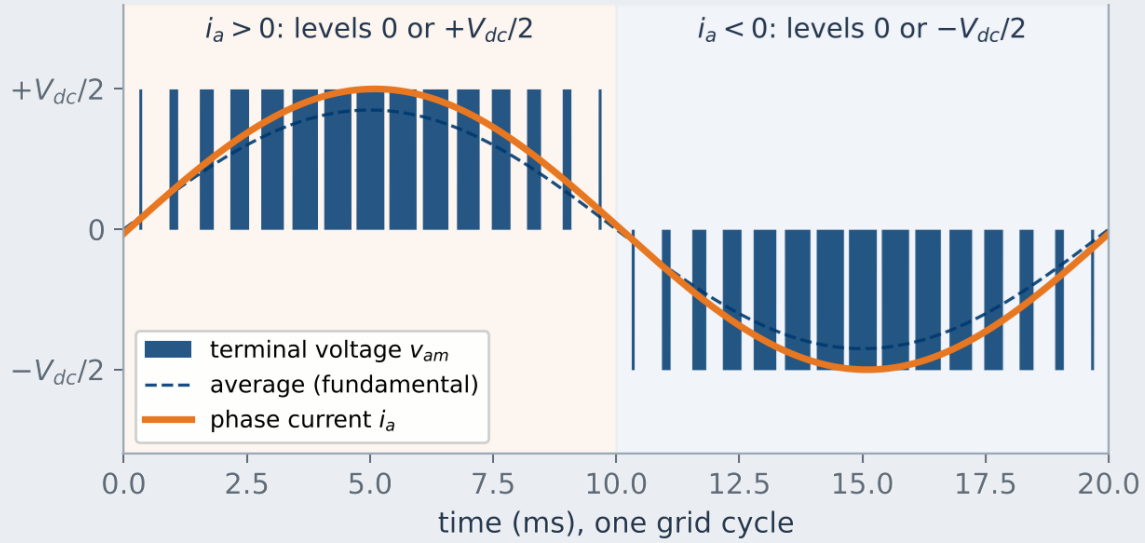

Fig. 3. Illustrative phase-a terminal voltage over one grid cycle: three levels, set by the switch and the current sign.

Switch ON
Phase tied to the midpoint m: $v_{am} = 0$; the inductor current builds up (boost action)

Switch OFF, $i_a > 0$
Current flows through the upper diode into C_1: $v_{am} = +V_{dc}/2$

Switch OFF, $i_a < 0$
Current flows through the lower diode from C_2: $v_{am} = -V_{dc}/2$

- The controller picks ON or OFF; the **current direction picks the rail**
- C_1 and C_2 share V_{dc}; keeping their midpoint centred is **neutral-point (NPV) balancing**

Switching states depend on the current direction

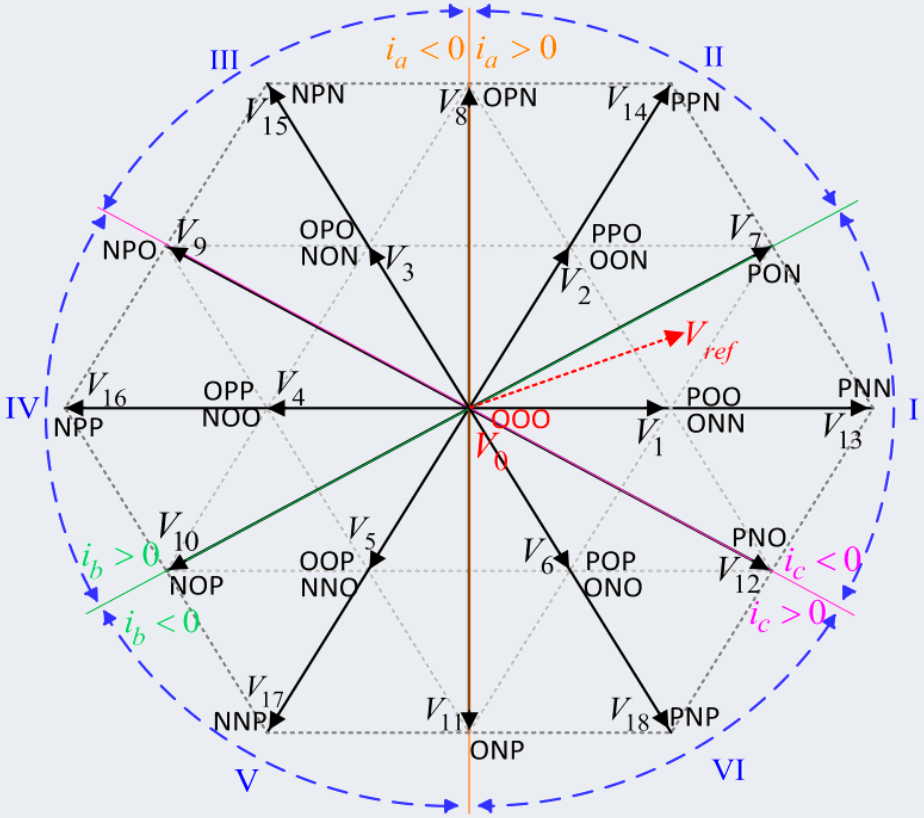

Fig. 4. Space vector diagram; the sector is set by the current polarity [2].

Table I. Switching states and terminal voltage [1], [2].

Phase current	State	S_x	V_{xm}
$i_x > 0$	P	0	$+V_{dc}/2$
$i_x > 0$ or < 0	O	1	0
$i_x < 0$	N	0	$-V_{dc}/2$

$$L_s \frac{di_x}{dt} = e_x - r_s\, i_x - V_{xm}, \qquad V_{xm} = \mathrm{sgn}(i_x)\,(1 - S_x)\,\frac{V_{dc}}{2}$$

- 27 combinations → **25 valid states → 19 distinct vectors**
- The rectifier can only apply voltages with the **same polarity as the current**
- Redundant small vectors (**POO / ONN**) charge C_1 or C_2 differently: the lever for neutral-point balancing

Four control ideas in plain words

PI control	Model predictive control	Optimal outer loop	Observer
Reacts to the error it has already seen; two gains trade speed against overshoot **In this talk:** The baseline in every paper	Predicts the next current for every switch choice and applies the best one **In this talk:** Inner loop of [1]–[3]	Sets the current reference for fast, well-damped DC-link control: LADRC rejects disturbances, LQR minimises error plus effort **In this talk:** LADRC [1], LQR [2]	Estimates what is not measured from what is: here, the phase currents themselves **In this talk:** MP-LESO [3]

- **"Optimal"** in the title = MPC with an LADRC [1] or LQR [2] outer loop: Parts 3 and 4
- **"Observer-based"** = the MP-LESO observer that replaces the current sensors [3]: Part 5

The cascaded control structure behind every design

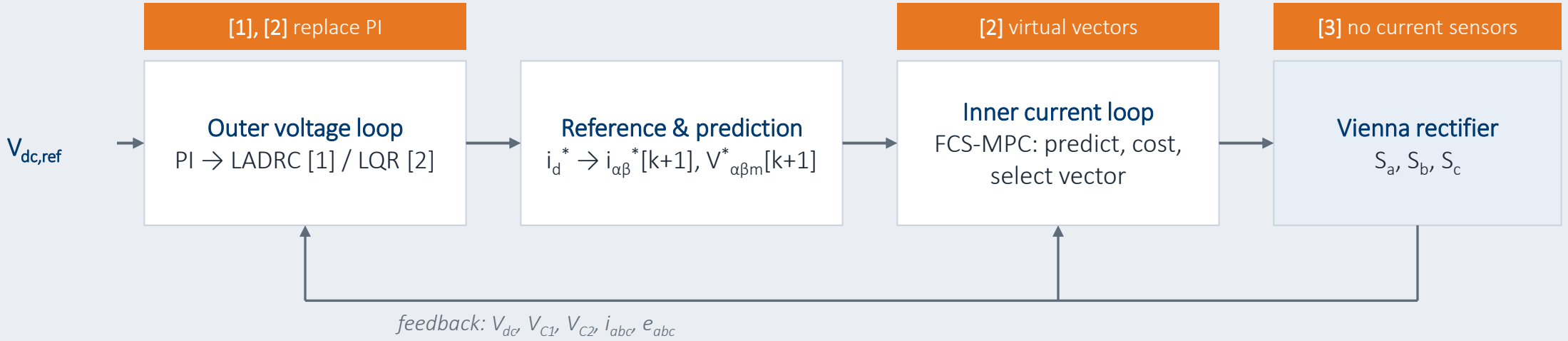

Fig. 5. Cascaded structure shared by [1]–[3]; orange tags mark where each paper changes it.

Inner loop: one-step prediction

$$i_{\alpha\beta}[k+1] = i_{\alpha\beta}[k] + \frac{T_s}{L_s}\left(e_{\alpha\beta}[k] - V_{\alpha\beta m}[k] - r_s\, i_{\alpha\beta}[k]\right)$$

- Evaluate every candidate vector with the discrete model; apply the one with the lowest cost g

Outer loop: sets the current amplitude

- Power balance: $P_{ac} = e_d i_d$ drives $\frac{1}{2}CV_{dc}^2$
- A slow or poorly damped i_d^* feeds an **imperfect reference** to the inner loop: harmonics and NPV ripple follow [1]

Three problems a good controller must solve

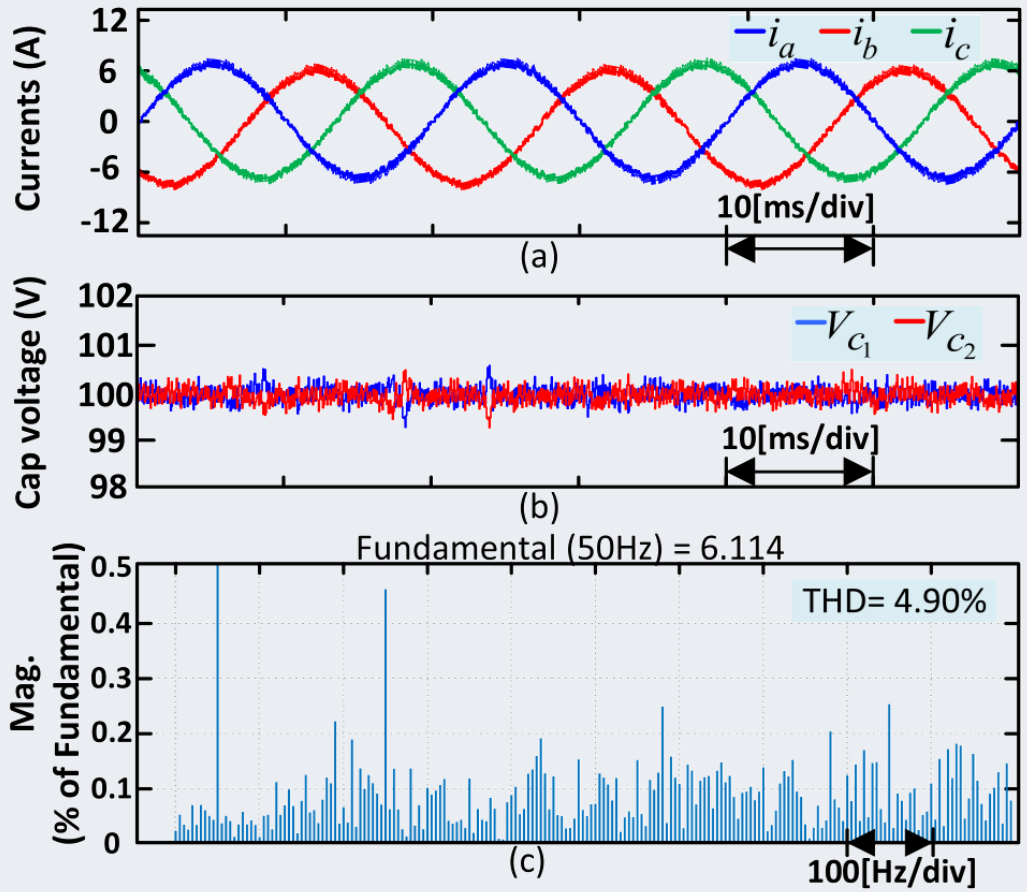

Fig. 6. Simulated PI + FCS-MPC baseline: (a) currents, (b) capacitor voltages, (c) FFT, THD 4.90 % [1].

1 Slow DC-link voltage control › Part 3

PI trades overshoot against settling time: **18.3–25 ms** to track a 30 V step [1], [2]; 3.6 V p-p capacitor ripple [1]

2 Input-current harmonics › Part 4

Few candidate vectors and an imperfect i_d^* leave low-order harmonics: **5.81 %** THD measured with PI + FCS-MPC [1]

3 Sensors and parameter drift › Part 5

Three current sensors add cost, noise and a failure point; L_s and C tolerances detune model-based control [3]

One test bench for all three studies

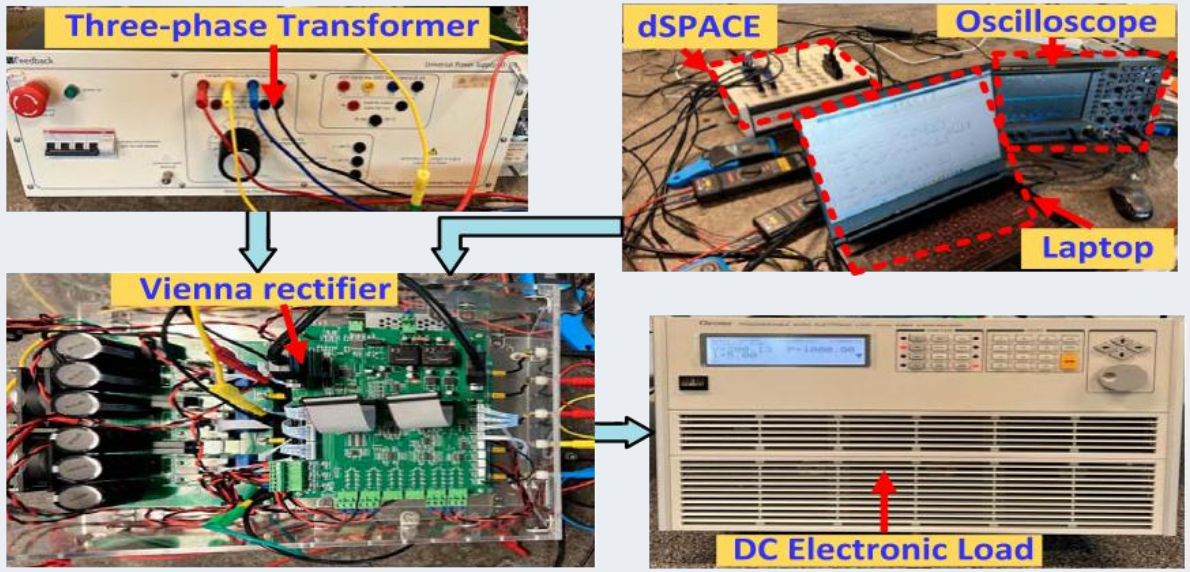

Fig. 7. Laboratory prototype: transformer, Vienna rectifier, dSPACE controller and DC electronic load [2].

- Same hardware, so gains from [1] to [3] are directly comparable
- Baselines: PI + FCS-MPC [1], PI + OSS-MPC [12] in [2], single-loop sensorless PR control [19] in [3]

Table II. Prototype parameters [1]–[3].

Parameter	Value
Grid voltage $e_{a,b,c}$	122 V peak, 50 Hz
DC-link voltage V_{dc}	200 V
DC-link capacitors C_1, C_2	1000 µF*
Load R_L (rated power)	40 Ω (1 kW)
Filter inductance L_s	5 mH
Sampling / switching frequency	20 kHz
Controller	dSPACE MicroLabBox 1202
DC load	Chroma 63800

* 1960 µF is listed in [1]

Part 2 of 6

What the literature offers

Modulation, predictive control, outer-loop alternatives and sensorless estimation

Thirty years of Vienna rectifier control

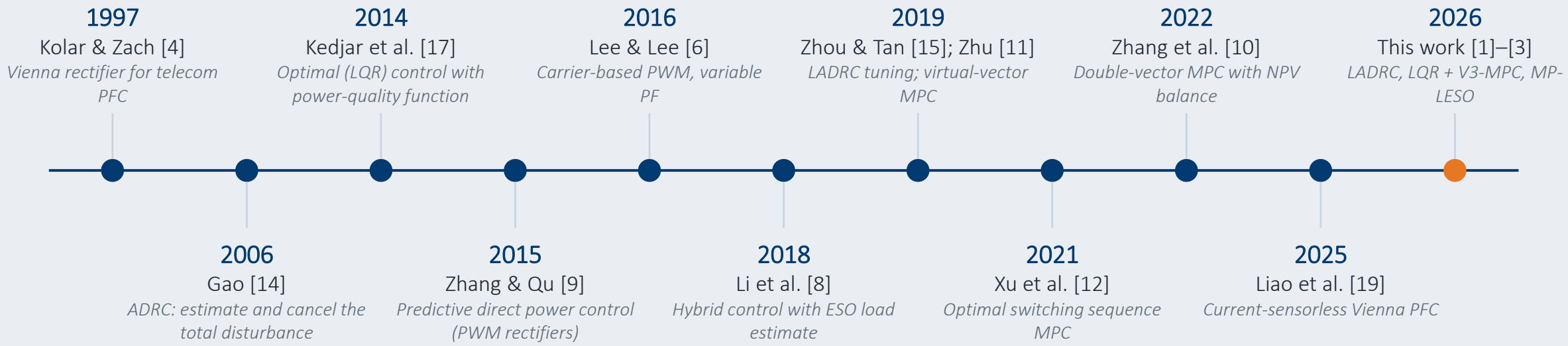

Fig. 8. Selected milestones in Vienna rectifier control.

Modulation versus predictive current control

Table III. Current-control approaches for the Vienna rectifier.

Approach	Strength	Limitation
Carrier-based PWM [6]	Simple, fixed f_{sw}	Switching loss; THD stays high
Discontinuous PWM [7]	Lower loss, NPV balance	Limited clamping range
Single-vector FCS-MPC [9]	No modulator, fast	Variable f_{sw}; needs high f_s or large L
Double-vector MPC [10]	Lower THD, NPV balance	Low THD only at heavy load
Optimised-vector MPC [13]	Fixed f_{sw}	Not all asymmetric sequences
Virtual-vector MPC [11]	Best reference synthesis	11–17 vectors: heavy computation
Optimal switching sequence [12]	Efficient (8 vectors/sector)	Coarse vector set: higher THD

Common thread

- Accuracy grows with the number of candidate vectors, and so does computation
- Every method above still uses a **PI controller** in the outer voltage loop [1], [2]

Replacing PI in the outer voltage loop

Table IV. Outer-loop voltage controllers.

Controller	Strength	Limitation
PI	Simple, well understood	Overshoot vs settling; weak disturbance rejection
SMC [18]	Robust to nonlinearity	Chattering distorts current; slow reaching
ADRC [14], [16]	ESO cancels lumped disturbance	Many nonlinear gains to tune
LADRC [15]	Bandwidth tuning	Fixed structure; tracking differentiator upset by DC disturbances
LQR [17]	Optimal, two weights (Q, R)	Rarely paired with advanced MPC

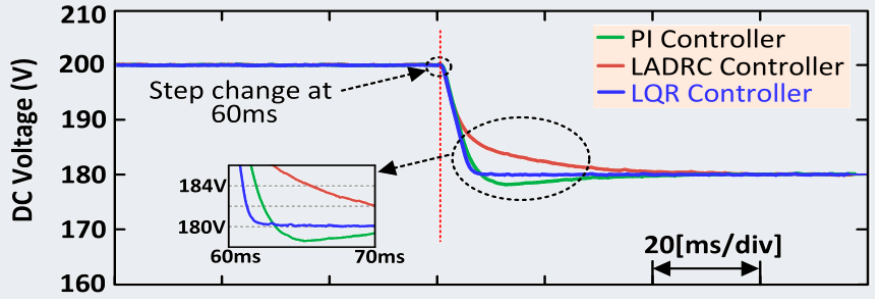

Fig. 9. DC-link reference step with PI, a standard LADRC and LQR outer loops on the same rectifier [2].

- PI undershoots; a standard LADRC avoids it but settles slowly
- LQR is fastest: Part 4. Making LADRC fast: Part 3

Sensorless control: voltage is well studied, current is not

Grid voltages e_{abc}
Measured in [3]

DC-link voltages V_{C1}, V_{C2}
Measured in [3]

Phase currents i_{abc}
Estimated by the MP-LESO observer in [3]

Fig. 10. Sensors needed by the controller in [3]; the current sensors are replaced by an observer.

Voltage-sensorless (well studied)

- ESO / LESO and direct-power grid-voltage estimators [20], [21], [24]
- Still rely on clean current measurement; parameter drift mostly ignored

Current-sensorless (sparse)

- Numerical current reconstruction [19], [22]; [19] uses a single voltage loop with PR control
- Good THD, but **380 ms** load transient and sensitivity to parameter mismatch [3]

Three gaps, three papers

	Gap	Contribution	
1	PI outer loop rejects disturbances poorly	**Improved LADRC + FCS-MPC**: RLS tracking and a predictive LESO replace PI	IEEE JESTIE, 2026 [1]
2	Few-vector MPC leaves harmonics; virtual vectors cost computation	**LQR + FS-V3-MPC**: sector-optimised virtual vectors, 7 candidates per region	IEEE TIE, 2026 [2]
3	Current-sensorless control lacks adaptivity and a current loop	**Hybrid MP-LESO observer**: RLS-adaptive LESO with model predictive current reconstruction	IEEE TPEL, 2026 [3]

Part 3 of 6

Optimal control I: improved LADRC

A faster, adaptive outer voltage loop with FCS-MPC inside [1]

LADRC: estimate the disturbance, then cancel it

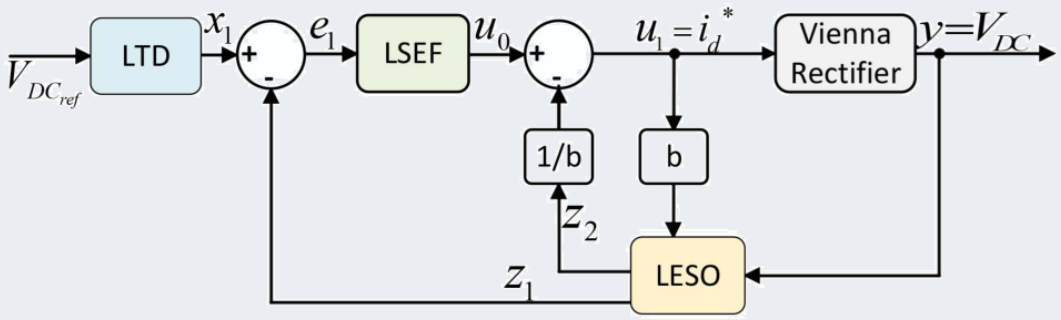

Fig. 11. Conventional first-order LADRC [1].

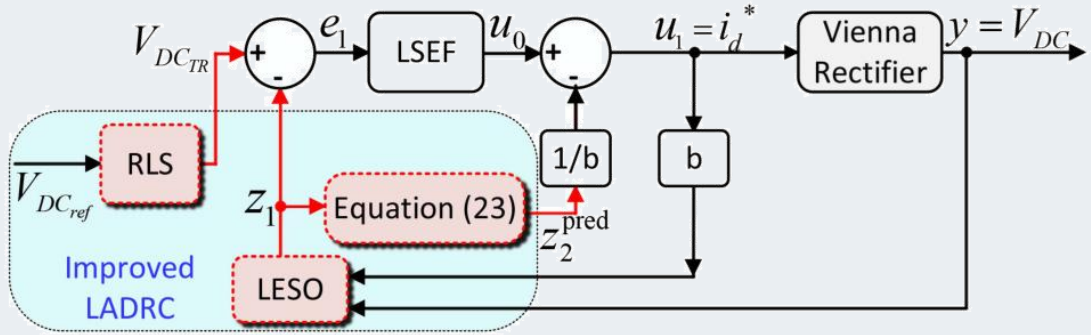

Fig. 12. Proposed improved LADRC: RLS tracking and predictive LESO (red) [1].

$$\dot{y} = b\,u + f, \quad y = V_{dc}^2, \quad b = \frac{4\sqrt{2}\,e_a}{C}, \quad f = -\frac{4V_{dc}^2}{CR_L}, \quad u = i_d$$

- Power balance turns the DC-link into $\dot{y} = bu + f$; all uncertainty is lumped into f
- The LESO estimates y (z_1) and f (z_2); the control law cancels f
- **Improvement 1:** recursive least squares (RLS) tracking replaces the linear tracking differentiator
- **Improvement 2:** predictive observer-aided control forecasts z_2 one step ahead

Inside the improved LADRC

Predictive LESO and control law

$$\dot{z}_1 = z_2 - \beta_1(z_1 - y) + b\,u, \qquad \dot{z}_2 = -\beta_2(z_1 - y)$$

$$z_2^{pred} = z_2 - \Delta t\,\beta_2(z_1 - y), \qquad i_d^* = k_p(x_1 - z_1) - z_2^{pred}/b$$

RLS-based reference tracking

$$V_{dc,TR}(t) = \theta_1 V_{dc,ref}(t) + \theta_2 V_{dc,ref}(t-1) + \theta_3 V_{dc,TR}(t-1)$$

- $\beta_1 = 692.82$, $\beta_2 = 1.2 \times 10^5$ ($\omega_0 = 346.41$ rad/s), $k_p = 100$
- Prediction step $\Delta t = 50$ µs ($\leq 1/f_{sw}$); RLS forgetting factor $\lambda \approx 0.99$

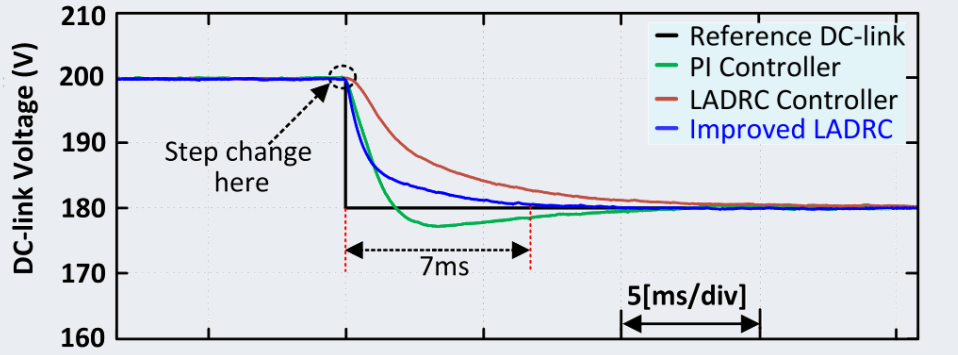

Fig. 13. Simulated DC-link reference tracking: PI, conventional LADRC and improved LADRC [1].

7.2 ms
tracking time

71 % faster
than a standard LADRC (25 ms)

Inner loop: FCS-MPC on a voltage-based cost

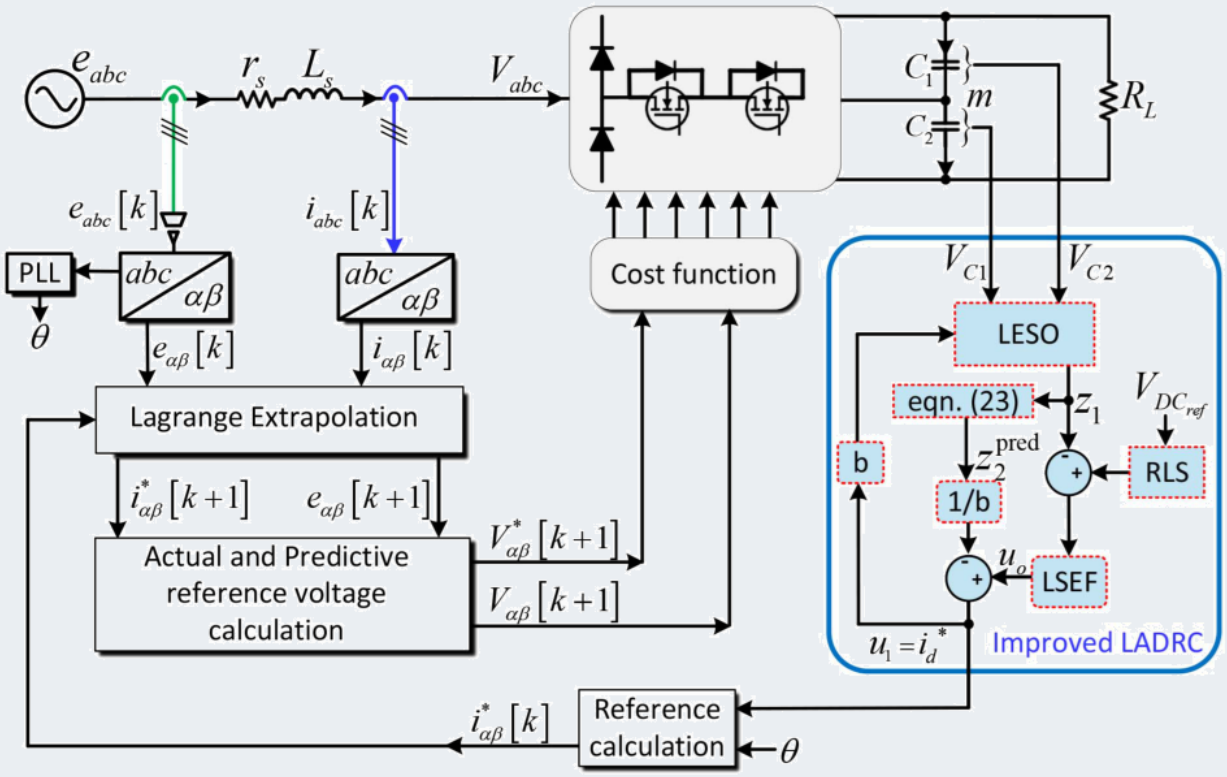

Fig. 14. Proposed control: improved LADRC outer loop and FCS-MPC inner loop [1].

$$g = \left[V^*_{\alpha m}(k+1) - V_{\alpha m}(k+1)\right]^2 + \left[V^*_{\beta m}(k+1) - V_{\beta m}(k+1)\right]^2$$

- Lagrange extrapolation predicts $i^*_{\alpha\beta}(k+1)$
- The model gives the reference voltage vector $V^*_{\alpha\beta m}(k+1)$, so the cost compares **voltages**
- Redundant vectors dropped: **25 → 19** evaluations per period
- NPV balanced by choosing **POO** when $V_{C1} > V_{C2}$, **ONN** otherwise: no weighting factor

Stability and design guidelines

Table V. Conventional versus improved LADRC [1].

Aspect	Conventional LADRC	Improved LADRC
Reference tracking	Linear tracking differentiator	RLS adaptive tracking
Disturbance estimate	z_2	Predicted z_2^{pred}
Tuning	ω_0, ω_c by hand	RLS (λ, P(0)) reduces effort
Stability proof	Bandwidth pole placement	Routh–Hurwitz incl. inner-loop lag
DC-link tracking	25 ms (as reported in [1])	**7.2 ms**

- Routh first column with inner-loop lag (τ = 50 µs), C −20 %, L_s −80 %: **all positive**
- Stable under the same variations used in the experiments

Design rules

- Observer bandwidth $\omega_0 = 3–10 \times \omega_c$
- k_p for a 10–100 Hz voltage-loop bandwidth
- $b = 4\sqrt{2}e_a/C$ and $k = 4/(CR_L)$ keep all coefficients positive
- Prediction horizon $\Delta t \leq 1/f_{sw}$
- RLS forgetting factor $\lambda \approx 0.99$

Results: cleaner current, steadier DC link

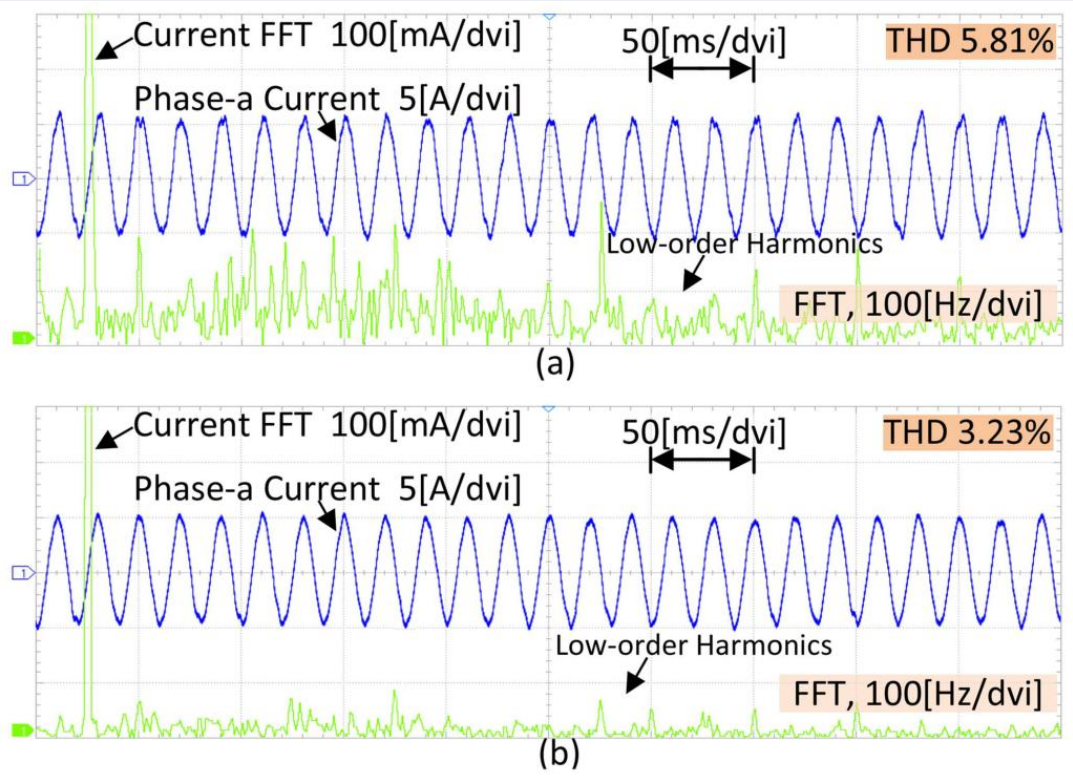

Fig. 15. Measured phase-a current and FFT: (a) PI + FCS-MPC, THD 5.81 %; (b) proposed, THD 3.23 % [1].

5.81 % → 3.23 %
input-current THD

3.6 V → 2.0 V
capacitor ripple (p-p)

18.3 → 7.2 ms
200 → 170 V step

15 % lower
THD than [12] at 1 kW

- The inner loop is unchanged; the gain comes from a **better reference**
- Low-order harmonics fall by 44 %

Faster tracking and robustness to load and inductance

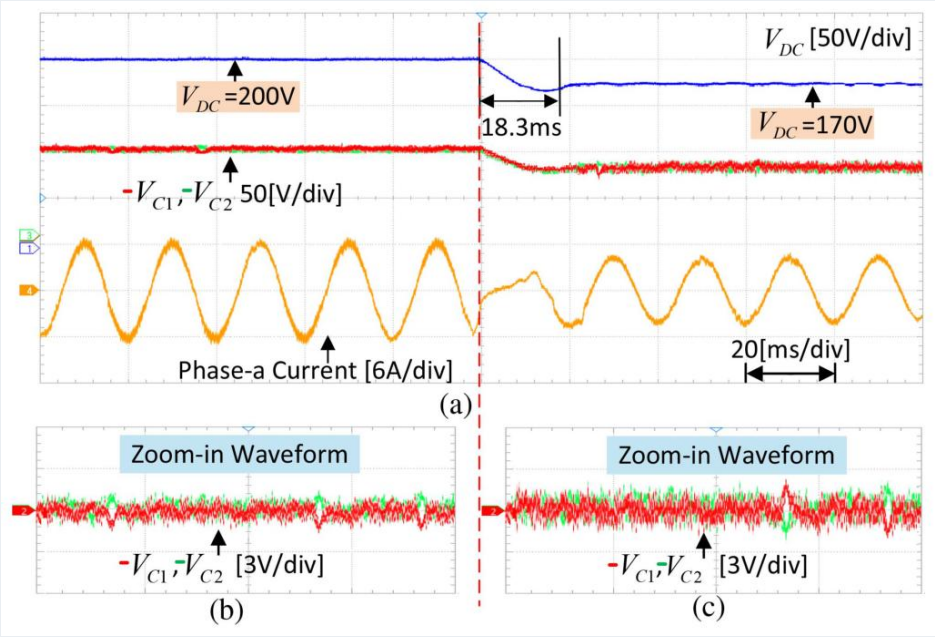

Fig. 16. PI + FCS-MPC: 18.3 ms to track 200 → 170 V [1].

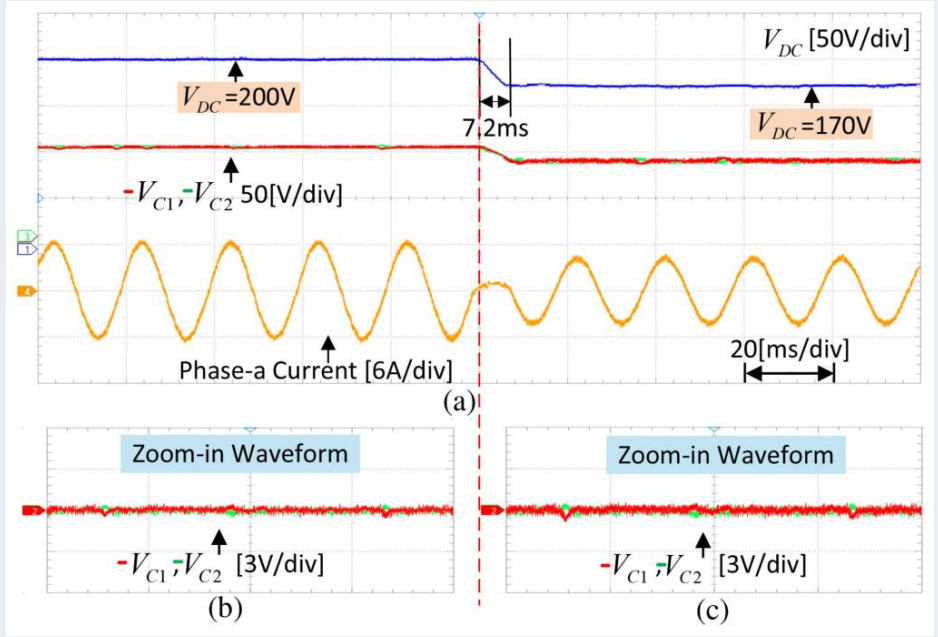

Fig. 17. Improved LADRC: 7.2 ms, lower capacitor ripple [1].

Load steps (20 %, 27 %)

THD 3.41 → 3.23 % with the proposed method vs 6.41 → 5.81 % with PI

Inductance cut (5 → 2 → 1 mH)

THD 3.23 → 4.40 → 4.91 %, stable throughout

Against the literature

2 V ripple vs 3.6–6.5 V; 7.2 ms vs 25–66 ms response [10], [12], [16], [26]

› Still open: the inner loop picks from a coarse vector set, which limits THD. Part 4 tackles it

Part 4 of 6

Optimal control II: LQR

An LQR voltage loop with sector-optimised virtual-vector MPC [2]

Closer candidate vectors, not more of them

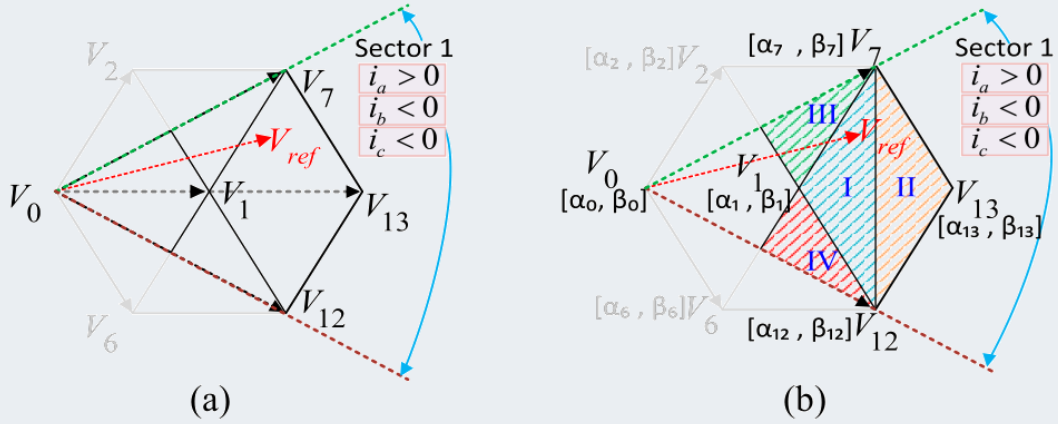

Fig. 18. Sector I: (a) conventional regions; (b) proposed regions I–IV [2].

Table VI. Candidate vectors per region of Sector I [2].

Region	Real vectors	Virtual vectors
I	V_1, V_{12}, V_7	V_{v6}, V_{v10}, V_{v11}, V_{v12}
II	V_7, V_{12}, V_{13}	V_{v11}, V_{v13}, V_{v14}, V_{v15}
III	V_1, V_7	V_{v1}, V_{v7}, V_{v8}, V_{v9}, V_{v17}
IV	V_1, V_{12}	V_{v2}, V_{v3}, V_{v4}, V_{v5}, V_{v16}

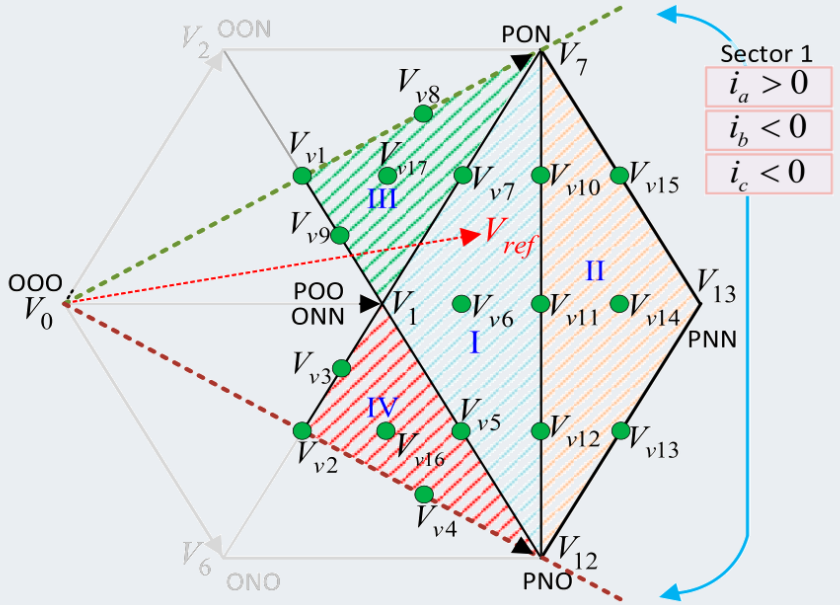

Fig. 19. Real (black) and virtual (green) voltage vectors in the Sector I regions [2].

- m > 0.577 in practice: **4 regions** per sector, not 6
- **7 candidates** per region vs 11–17 in [11]

Locating the reference and synthesising virtual vectors

Region identification: barycentric test

$$V_{ref} = a\,V_1 + b\,V_{12} + c\,V_7, \qquad a+b+c=1, \qquad 0 \le a,b,c \le 1$$

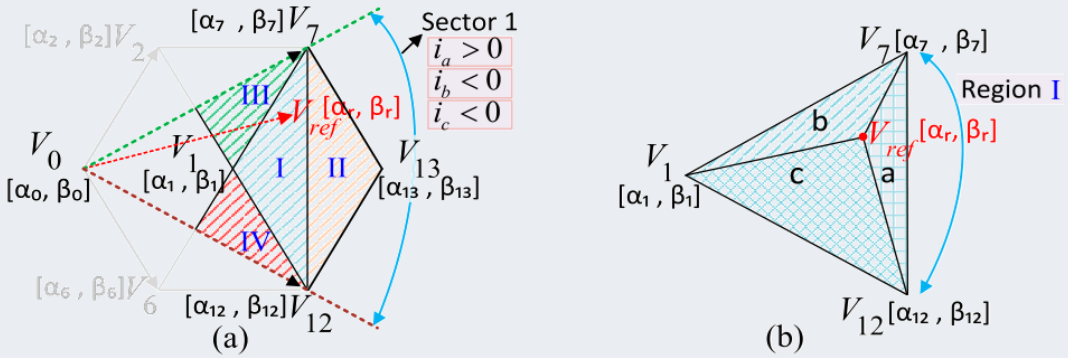

Fig. 20. (a) Sector I regions; (b) barycentric coordinates in Region I [2].

- Sector from atan2($V_{ref\beta}$, $V_{ref\alpha}$); region from **0 ≤ a, b, c ≤ 1**
- Algebraic comparisons only: no iterative search

Virtual vectors within one T_s

$$V_v\,T_s = V_I\,t_I + V_{II}\,t_{II} \quad \Rightarrow \quad V_{v4} = \tfrac{1}{4}V_1 + \tfrac{1}{4}V_6 + \tfrac{1}{2}V_{12}$$

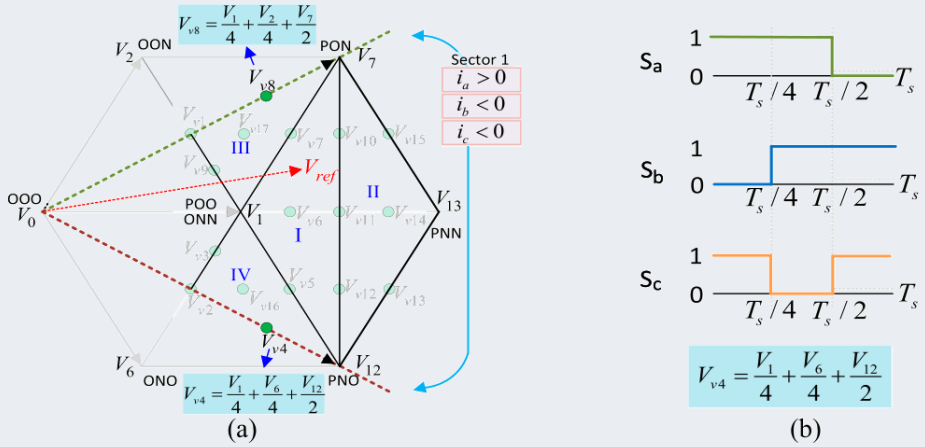

Fig. 21. (a) Virtual vector synthesis; (b) switching sequence for V_{v4} [2].

- Constant switching frequency: THD falls from **better synthesis**, not faster switching

LQR for the DC-link voltage

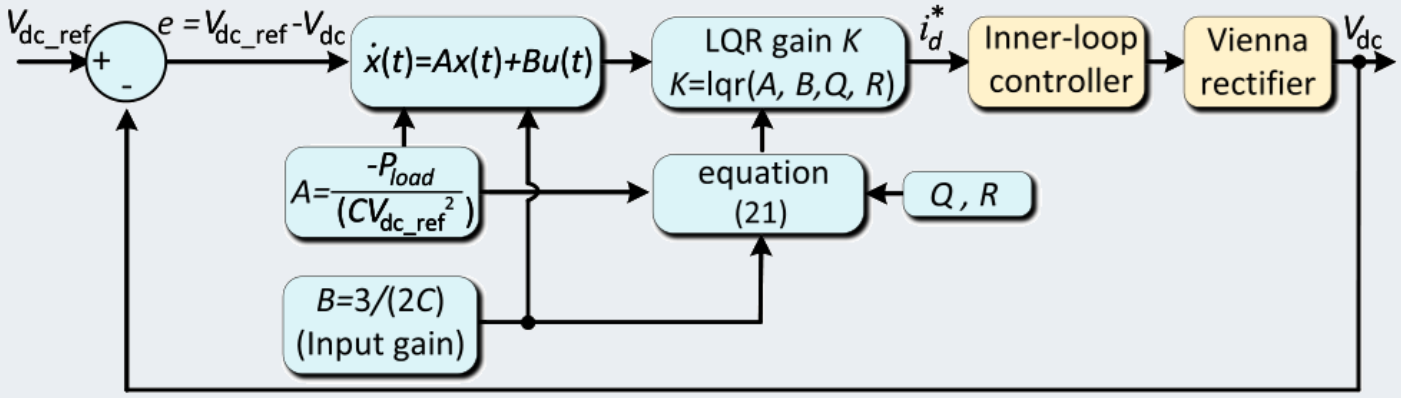

Fig. 22. LQR outer-loop controller [2].

- **Two weights instead of PI gains:** Q penalises voltage error, R penalises current demand
- Q = 815, R = 0.4 from practical tuning; **K** from the Riccati equation
- Current control in the stationary αβ frame: **no PLL** in the voltage loop
- Faster tracking and better disturbance rejection than PI (preview on the Part 2 slide)

Small-signal model, cost and gain

$$\Delta \dot{V}_{DC} = -\frac{P_{load}}{C\,V_{DC,\,ref}^2}\,\Delta V_{DC} + \frac{3}{2C}\,\Delta i_d$$

$$J = \int_0^{\infty} (Q\,x^2 + R\,u^2)\,dt, \qquad 2AP - \frac{B^2P^2}{R} + Q = 0$$

$$K = R^{-1}BP, \qquad i_d^* = -K\,\Delta V_{DC}$$

The complete controller, and why it stays stable

Is it stable? Yes, with margin

- An **energy-like (Lyapunov) function** of the current and voltage errors always decreases, so errors die out
- The fast predictive inner loop removes current errors first; the LQR then settles the DC link
- Proof details in the backup slides

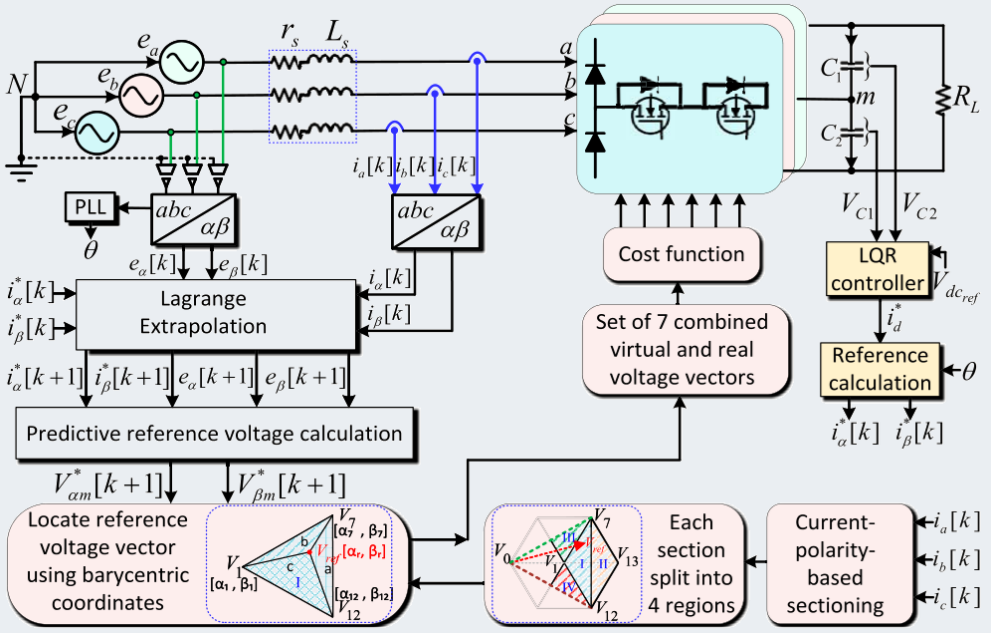

Fig. 23. Complete scheme: LQR outer loop with FS-V3-MPC inner loop [2].

−80 % L_s still stable	**±20 % C** still stable	**20–80 Ω R_L** still stable

Results: 2.01 % THD and 6.5 ms tracking

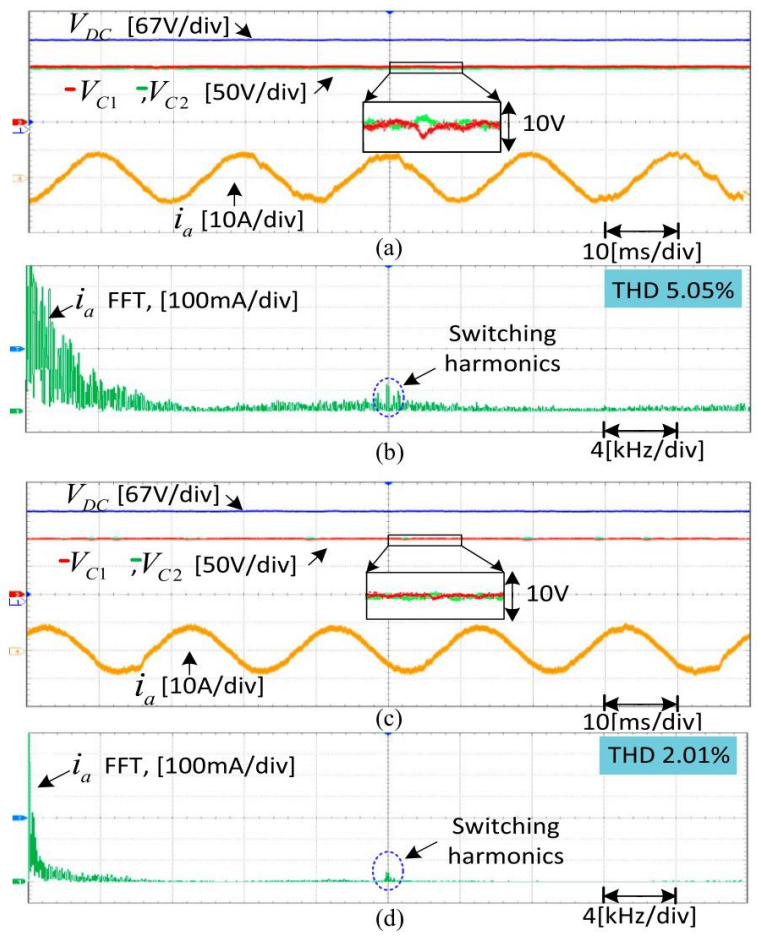

Fig. 24. Steady state: (a, b) PI + OSS-MPC, THD 5.05 %; (c, d) proposed, THD 2.01 % [2].

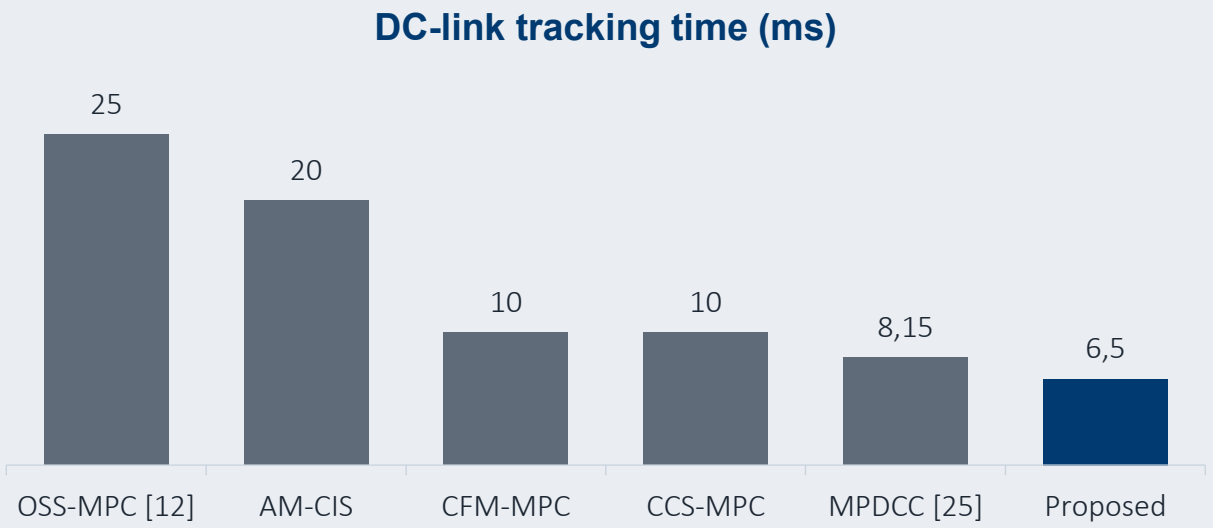

Fig. 25. Measured DC-link tracking time of MPC algorithms, as compared in [2].

−60 %
THD vs OSS-MPC

74 % faster
than PI (25 ms)

4.5 µs
execution time

Robust to load, unbalance, grid and inductance changes

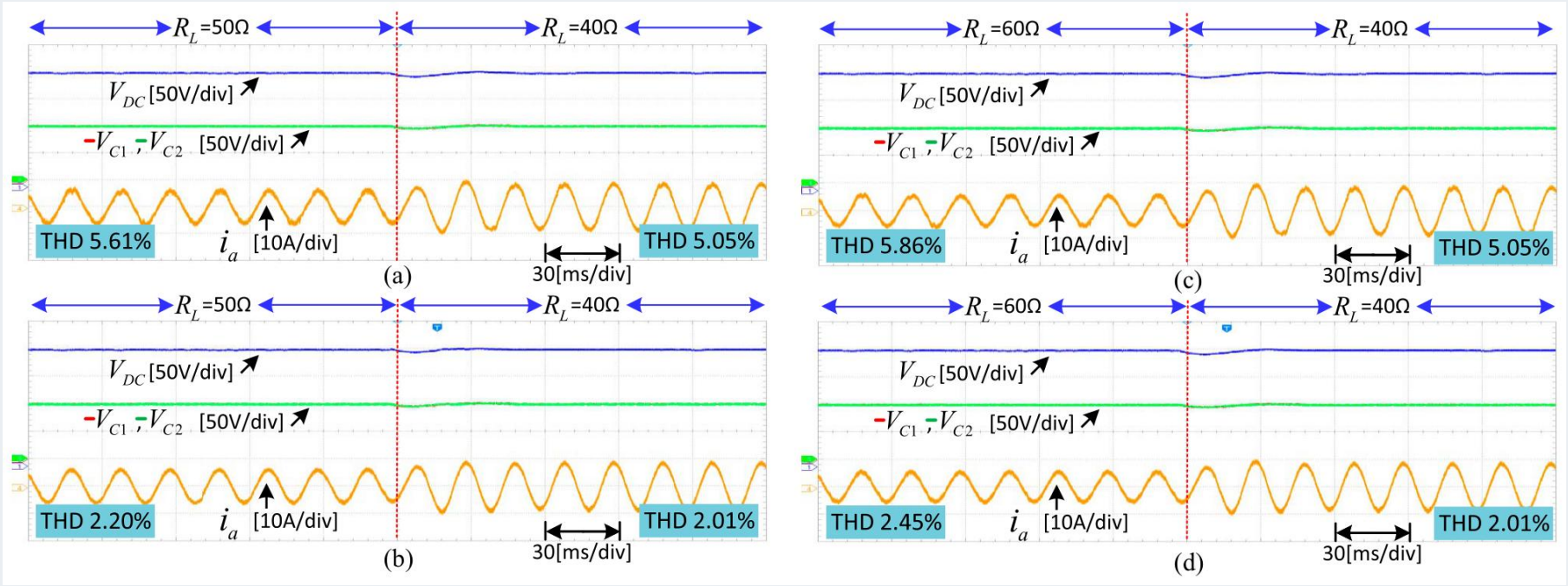

Fig. 26. Load steps: (a, c) OSS-MPC, THD 5.61/5.86 → 5.05 %; (b, d) proposed, THD 2.20/2.45 → 2.01 % [2].

Unbalanced DC load

15 Ω / 25 Ω split load: NPV stays balanced, current regulated

Grid voltage +2 to +10 %

No PLL in the voltage loop: currents stay sinusoidal

Inductance cut (5 → 2 → 1 mH)

THD 2.01 → 3.50 → 4.14 %, stable throughout

› Still open: every controller so far needs three current sensors. Part 5 removes them

Part 5 of 6

Observer-based control

A model predictive hybrid observer that removes the current sensors [3]

Why go current-sensorless?

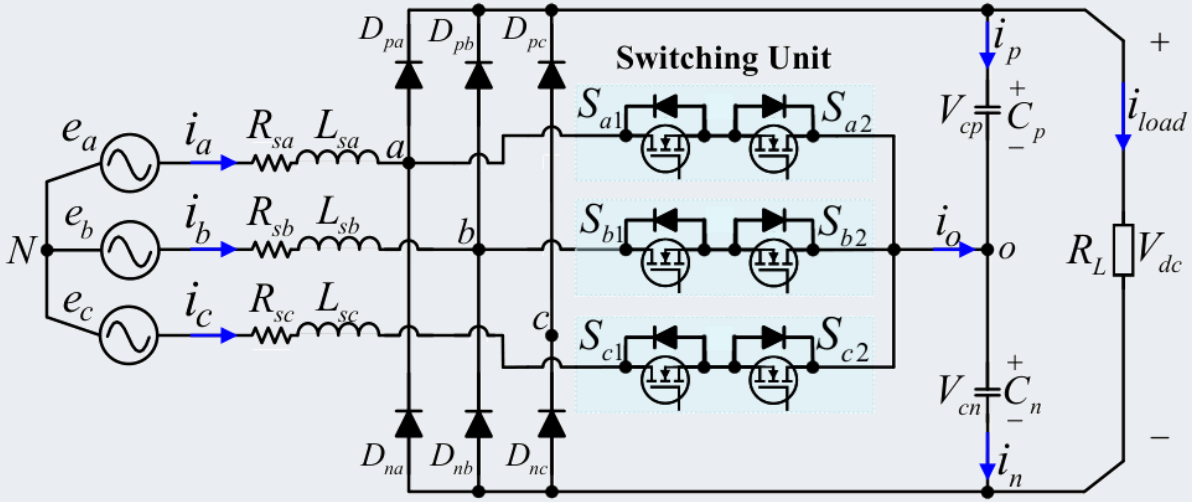

Fig. 27. Vienna rectifier with split DC link as modelled in [3].

- Measured: e_{abc}, V_{cp}, V_{cn}; i_{load} is computed from V_{dc} and R_L
- Estimated: i_{abc} and a lumped disturbance f_x

Why remove them

- Sensors are a **non-negligible share** of hardware cost [3]
- Sensor noise propagates through **both loops**
- An observer gives a **backup** if a sensor fails

What it must achieve

- Accurate enough to close a **current loop**, not just a voltage loop
- Robust to L, C and R_L drift

The hybrid MP-LESO observer

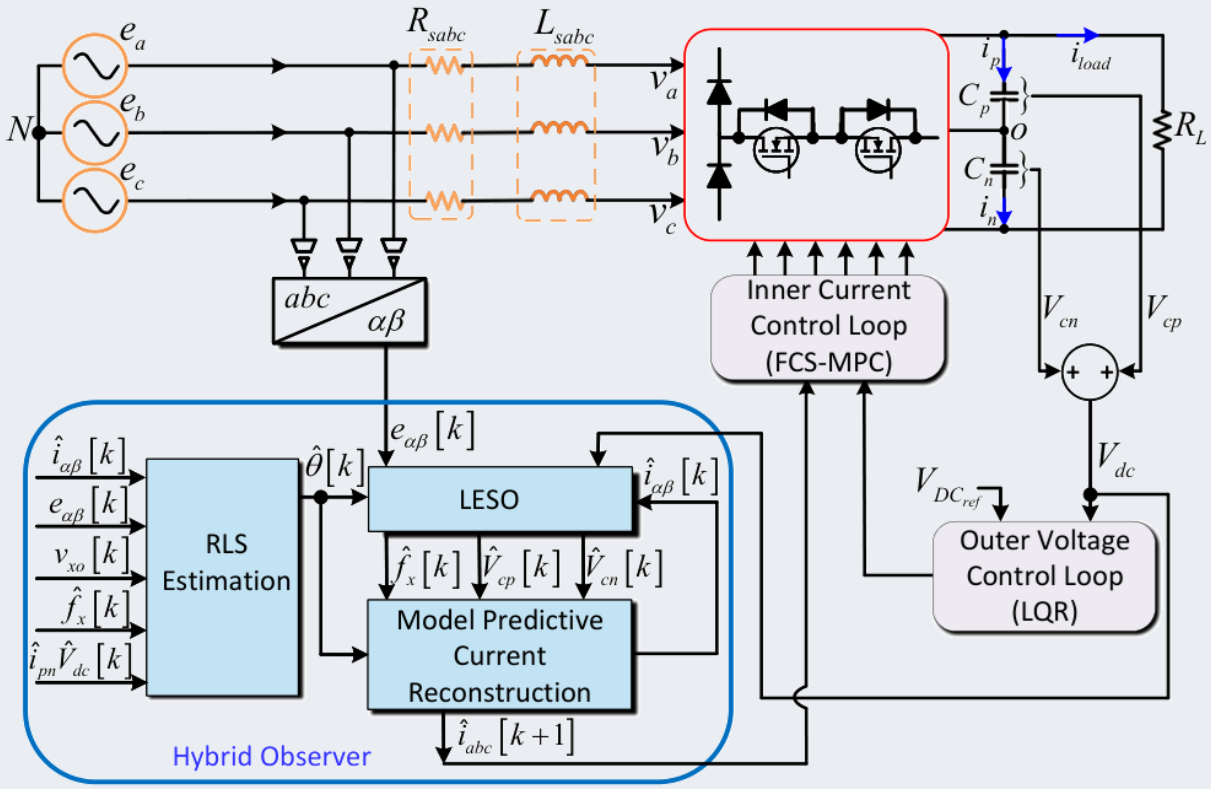

Fig. 28. Overall control scheme with the hybrid MP-LESO observer (blue) [3].

1 Measure
V_{dc}, e_{abc}; compute $y = V_{dc}i_{load}/R_L$

2 LESO update
estimate f_x, V_{cp}, V_{cn} from the DC power error

3 RLS adaptation
update $\theta = [R/L, 1/L, \lambda, 1/C_p, 1/C_n]$

4 MP reconstruction
predict $i_{abc}[k+1]$ from f_x and the adapted θ

5 Close the loop
FCS-MPC uses the estimate in place of a sensor

Observer equations and online adaptation

Adaptive LESO (DC side)

$$\dot{\hat{x}} = A\hat{x} + B\hat{u} + L(y - \hat{y}), \qquad \hat{x} = [\hat{f}_x,\ \hat{V}_{cp},\ \hat{V}_{cn}]^T, \qquad y = V_{dc}\, i_{load}/R_L$$

RLS parameter vector

$$\theta = \left[\hat{R}/\hat{L},\ 1/\hat{L},\ \lambda,\ 1/\hat{C}_p,\ 1/\hat{C}_n\right]^T$$

Model predictive current reconstruction

$$\hat{i}_{\alpha\beta}[k+1] = \hat{i}_{\alpha\beta}[k] + T_s\left(-\frac{\hat{R}}{\hat{L}}\hat{i}_{\alpha\beta}[k] + \frac{1}{\hat{L}}(e_{\alpha\beta}[k] - v_{\alpha\beta o}[k]) + \hat{f}_{\alpha\beta}[k]\right)$$

Lumped disturbance f_x

Device voltage drops, NPV second-harmonic ripple and nonlinear terms in one estimate

RLS adaptation

Forgetting factor 0.98–0.995; P(0) ≥ diag(10^4, …, 10^6) for fast, smooth convergence

MP step

One-step horizon, no extra tuning; sgn(î) sets the terminal voltage

Does the estimate converge? Stability and design rules

Is the estimate reliable? Yes

- The estimation error **always shrinks** (Lyapunov proof), even with −80 % L, ±20 % C and 20–80 Ω load
- Observer bandwidth **5024 rad/s**, well above the slower adaptation

Design rules

- Place all LESO poles at $-\omega_o$; ω_o = 8–15 × grid frequency or more
- RLS λ = 0.98–0.995; regressor persistently exciting in normal operation

Table VII. Current-sensorless methods compared [3].

Aspect	Method in [19]	MP-LESO [3]
Structure	Single voltage loop, feed-forward	Dual loop + hybrid observer
Tuning	Heuristic, offline	Bandwidth + online RLS
Stability	Small-signal / Bode	Lyapunov with ±20 % C, −80 % L
Load transient	380 ms	**35 ms**
THD	< 5 %	**1.90 %**

Results: 1.90 % THD without current sensors

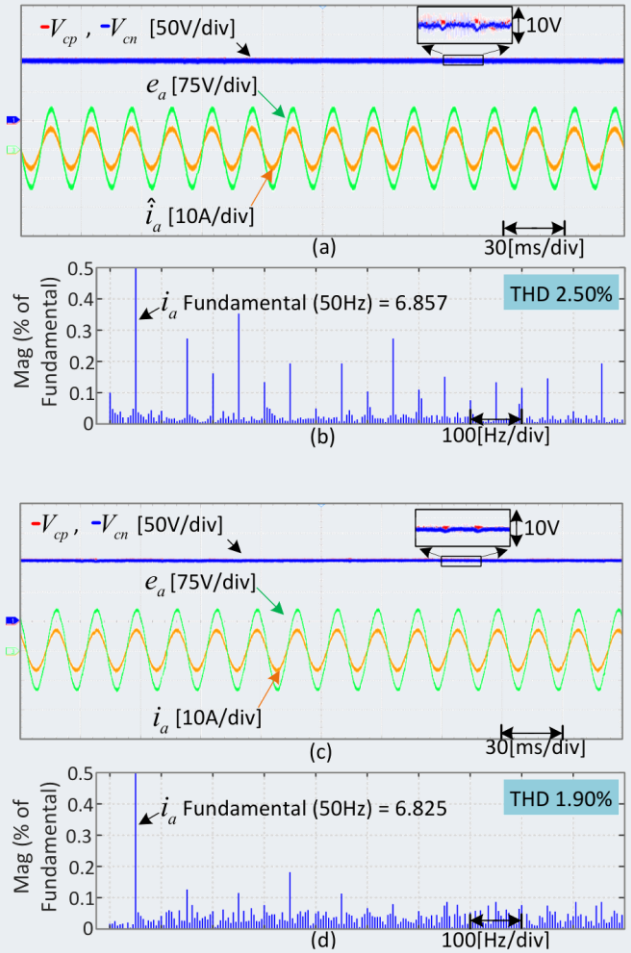

Fig. 29. Steady state: (a, b) method of [19], THD 2.50 %; (c, d) proposed, THD 1.90 % [3].

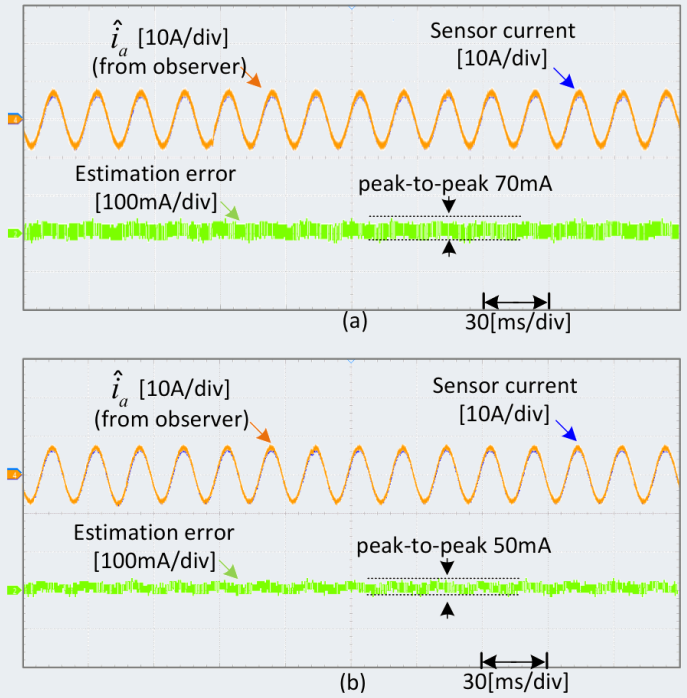

Fig. 30. Observer vs validation sensor: (a) [19], 70 mA p-p error; (b) proposed, 50 mA [3].

2.50 % → 1.90 %
THD, −24 %

70 → 50 mA
estimation error p-p, −28 %

5.2 µs
execution time per cycle

Dynamics and robustness without current sensors

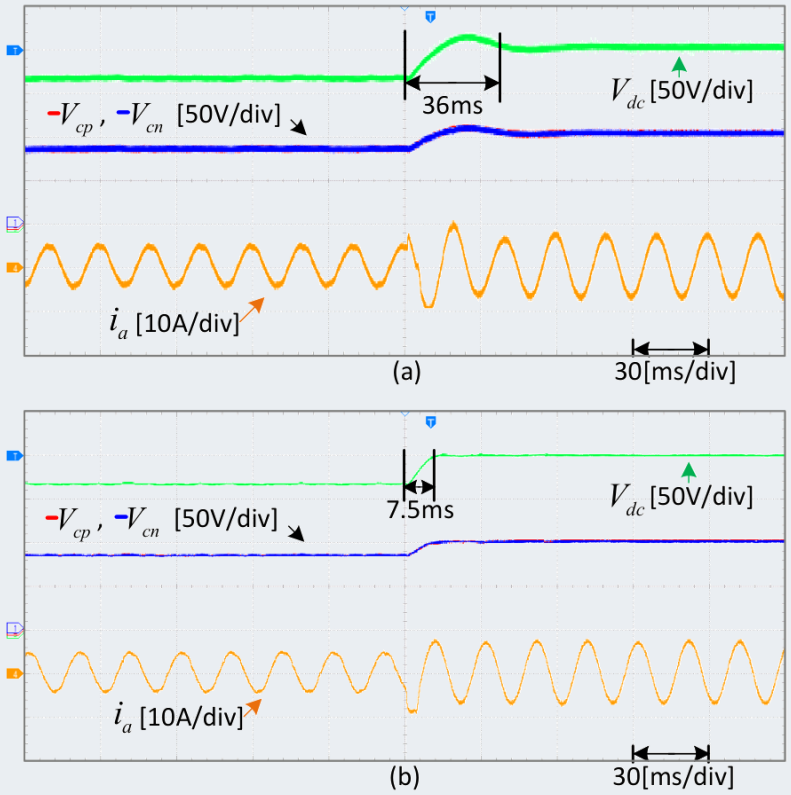

Fig. 31. DC-link step 170 → 200 V: (a) [19], 36 ms; (b) proposed, 7.5 ms [3].

Start-up 42 ms; THD < 5 % down to 100 W (4.85 %)

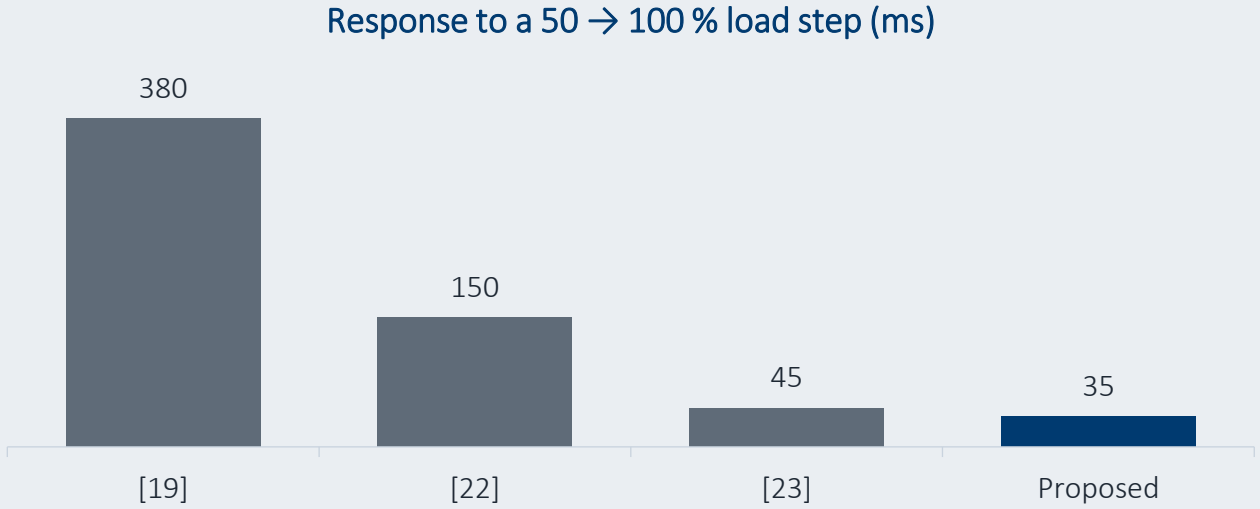

Fig. 32. Measured load-step response time of current-sensorless methods, as compared in [3].

Grid imbalance

Phase B at 70 % with harmonics: THD 2.10 % vs 2.86 % [19]

Mismatched capacitors

C_p = 1070 µF, C_n = 1000 µF: NPV re-balanced in 22 ms

› Next: how the three methods compare, and which to choose (Part 6)

Part 6 of 6

Comparison and design guidance

What each method buys you, and how to choose

Three controllers on one 1 kW prototype

Table VIII. Summary of the three methods (experimental, unity power factor, 1 kW).

	Optimal I: LADRC [1]	Optimal II: LQR [2]	Observer-based [3]
Outer voltage loop	Improved LADRC	LQR (Q = 815, R = 0.4)	Dual loop with MP-LESO
Inner current loop	FCS-MPC, 19 vectors	FS-V3-MPC, 7 per region	FCS-MPC on estimated current
Current sensors	3	3	**0**
Input-current THD	3.23 % (5.81 %)	2.01 % (5.05 %)	**1.90 %** (2.50 %)
DC-link step tracking	7.2 ms (18.3 ms)	**6.5 ms** (25 ms)	7.5 ms (36 ms)
Execution time	—	**4.5 µs**	5.2 µs
THD at L_s = 1 mH	4.91 %	**4.14 %**	4.71 %*
Stability proof	Routh–Hurwitz	Lyapunov + sensitivity	Lyapunov (perturbed)

Baseline in brackets: PI + FCS-MPC [1]; PI + OSS-MPC [12] in [2]; sensorless method of [19] in [3]. * Value read from Fig. 10(f) of [3].

Where the results sit against the literature

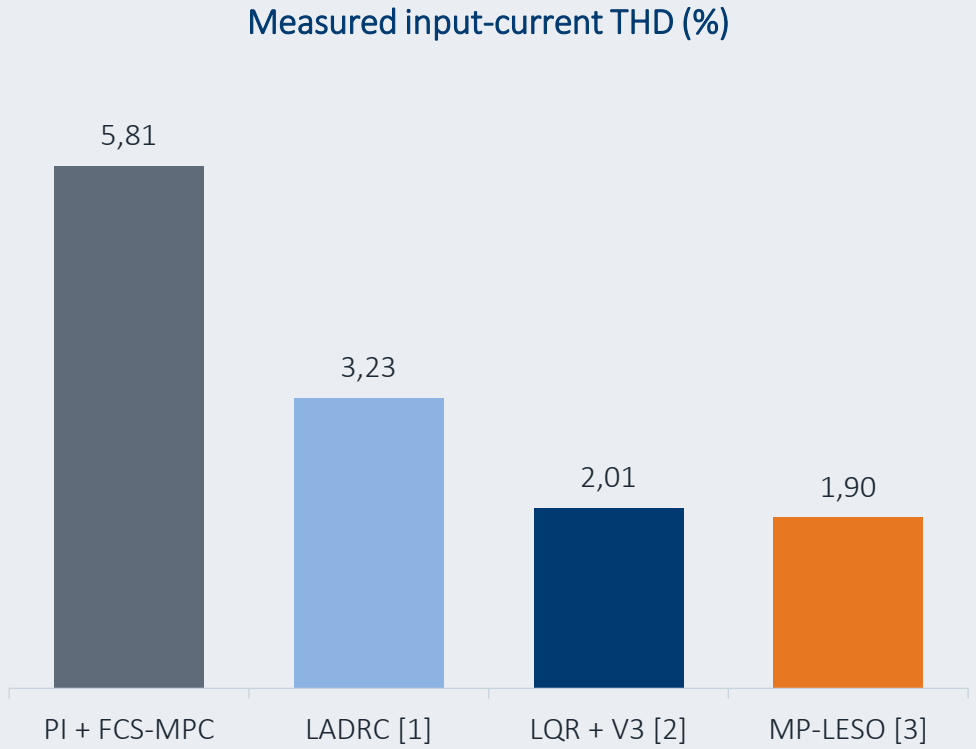

Fig. 33. THD on the same 1 kW prototype, baseline to [3].

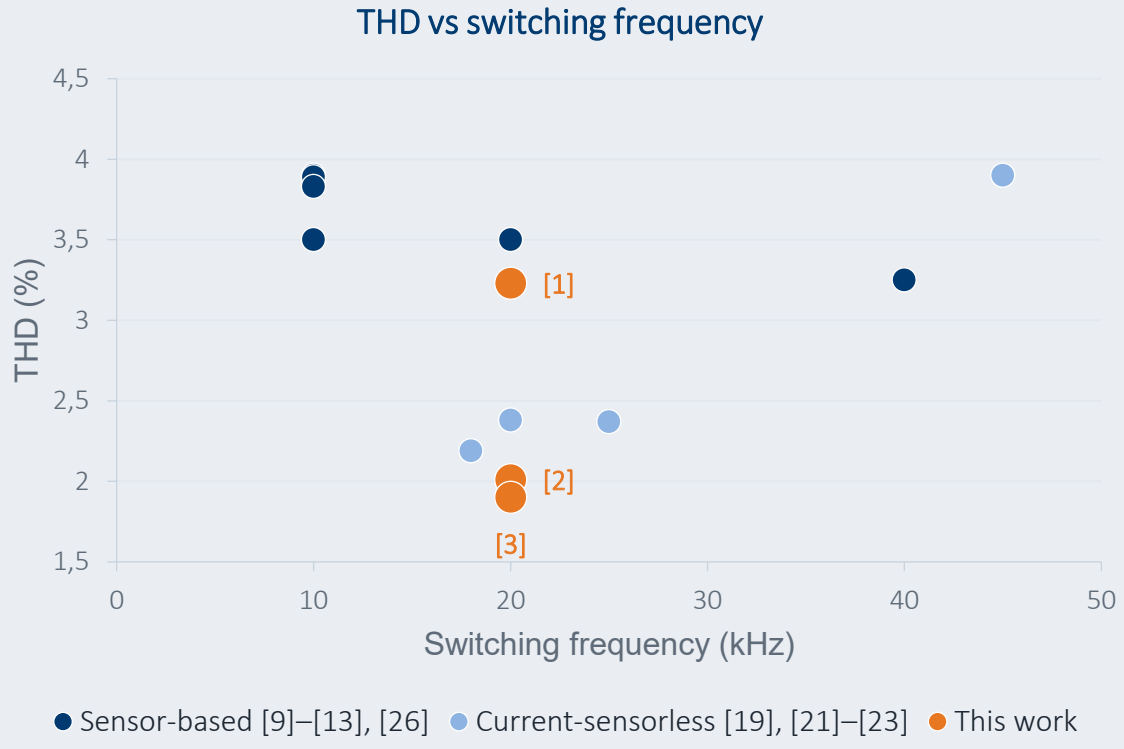

Fig. 34. Reported experimental THD of Vienna rectifier controllers [1]–[3].

Literature values as reported in the comparison tables of [1]–[3]; ratings range from 0.8 to 5 kW.

Choosing a method

Improved LADRC + FCS-MPC [1]	LQR + FS-V3-MPC [2]	MP-LESO observer [3]
Choose when › Load and parameter disturbances dominate › You want bandwidth-style tuning › You keep a standard FCS-MPC inner loop	Choose when › Lowest THD at fixed f_{sw} matters › Computation is tight (4.5 µs) › Grid voltage varies (no PLL in the loop)	Choose when › Sensor cost or space is limited › Fault tolerance needs a backup current signal › L, C and load drift online

› The pieces combine: [3] already runs on the same dual-loop structure, so the observer can sit under either outer loop

Design rules summarised

Table IX. Practical rules for optimal and observer-based Vienna rectifier control.

#	Rule	Why	Source
1	Balance NPV with redundant small vectors (POO / ONN), not a weighting factor	No weight to tune; fewer evaluations	[1], [2], [10]
2	Use a voltage-based cost and drop redundant vectors (25 → 19)	Lower computation	[1]
3	With m > 0.577, use 4 regions per sector and 7 candidates	Accuracy at low cost	[2]
4	Synthesise virtual vectors from real vectors within one T_s	Constant switching frequency	[2], [11]
5	LADRC observer bandwidth $\omega_0 = 3–10 \times \omega_c$; $\Delta t \leq 1/f_{sw}$	Fast estimation without noise	[1], [15]
6	LESO poles at $-\omega_o$ ($3\omega_o$, $3\omega_o^2$, ω_o^3); RLS $\lambda = 0.98–0.995$	Clean damping; smooth adaptation	[3]
7	Tune LQR with Q (voltage error) and R (current demand)	Two intuitive weights replace PI gains	[2]
8	Check stability with ±20 % C, −80 % L_s, 0.5–2 × R_L	Prototypes drift	[1]–[3]

A design workflow for Vienna rectifier control

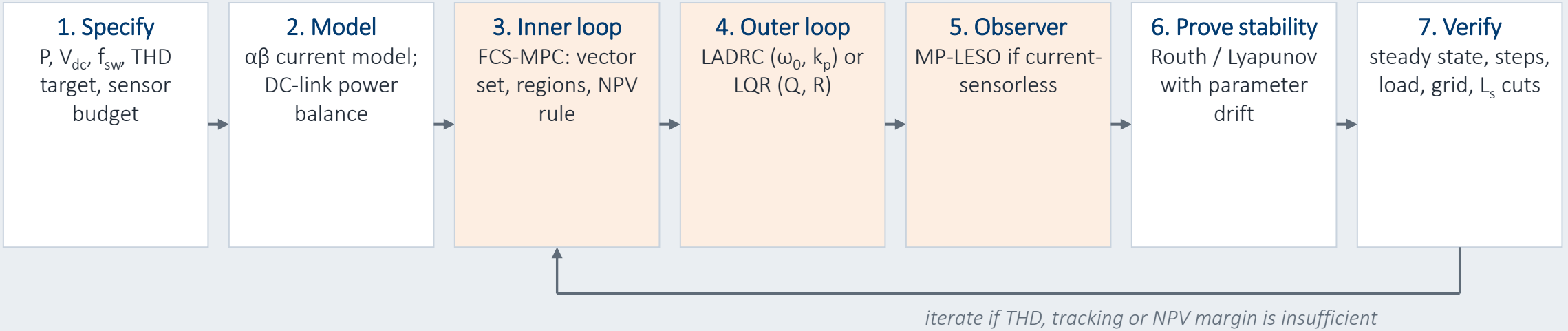

Lab tips

- Simulate with the exact prototype parameters before hardware
- Compare against a baseline on the **same** bench
- Step both ways (200 → 170 → 200 V) and cut L_s deliberately

Open questions

- T-type, NPC and other multilevel converters [1]–[3]
- Unbalanced, nonlinear and LCL grid-tied operation [2], [3]
- Adaptive or AI-based tuning; low-cost processors [2], [3]

Key takeaways

1	PI is the weak link	In a cascaded Vienna rectifier controller, the outer PI loop limits both DC-link dynamics and current quality.
2	A better outer loop cleans the current	Improved LADRC (RLS + predictive LESO): THD 5.81 → 3.23 %, tracking 18.3 → 7.2 ms.
3	LQR and closer vectors go further	LQR with sector-optimised virtual-vector MPC: 2.01 % THD, 6.5 ms tracking, 4.5 µs execution.
4	An observer can replace the sensors	The hybrid MP-LESO observer reconstructs the currents: 1.90 % THD with no current sensors.
5	Prove robustness, then test it	Routh–Hurwitz and Lyapunov analyses, confirmed with −80 % L_s, load steps and grid disturbances.

References (1/2)

[1] T. Uzzaman, T. Fernando, H. H. Iu and X. Zhang, "An improved linear active disturbance rejection control with FCS-MPC for three phase three-level Vienna rectifier," IEEE J. Emerg. Sel. Topics Ind. Electron., vol. 7, no. 2, pp. 591–603, Apr. 2026, doi: 10.1109/JESTIE.2025.3647450.

[2] T. Uzzaman, T. Fernando, H. H. Iu and X. Zhang, "An advanced predictive control strategy for current harmonic suppression in three-phase three-level Vienna rectifier," IEEE Trans. Ind. Electron., 2026, doi: 10.1109/TIE.2026.3684165.

[3] T. Uzzaman, T. Fernando, H. H. Iu and X. Zhang, "A model predictive hybrid observer for current sensorless PFC operation of three-phase three-level Vienna rectifier," IEEE Trans. Power Electron., 2026, doi: 10.1109/TPEL.2026.3699625.

[4] J. W. Kolar and F. C. Zach, "A novel three-phase utility interface minimizing line current harmonics of high-power telecommunications rectifier modules," IEEE Trans. Ind. Electron., vol. 44, no. 4, pp. 456–467, Aug. 1997.

[5] M. Zhang, Y. Yuan, X. Sun, Y. Zhang and X. Li, "Harmonic resonance suppression strategy of the front-end Vienna rectifier in EV charging piles," IEEE Trans. Power Electron., vol. 38, no. 1, pp. 1036–1053, Jan. 2023.

[6] J.-S. Lee and K.-B. Lee, "A novel carrier-based PWM method for Vienna rectifier with a variable power factor," IEEE Trans. Ind. Electron., vol. 63, no. 1, pp. 3–12, Jan. 2016.

[7] L. Zhang et al., "A modified DPWM with neutral point voltage balance capability for three-phase Vienna rectifiers," IEEE Trans. Power Electron., vol. 36, no. 1, pp. 263–273, Jan. 2021.

[8] X. Li, Y. Sun, H. Wang, M. Su and S. Huang, "A hybrid control scheme for three-phase Vienna rectifiers," IEEE Trans. Power Electron., vol. 33, no. 1, pp. 629–640, Jan. 2018.

[9] Y. Zhang and C. Qu, "Model predictive direct power control of PWM rectifiers under unbalanced network conditions," IEEE Trans. Ind. Electron., vol. 62, no. 7, pp. 4011–4022, Jul. 2015.

[10] H. Zhang et al., "Three-layer double-vector model predictive control strategy for current harmonic reduction and neutral-point voltage balance in Vienna rectifier," IEEE Trans. Transport. Electrific., vol. 8, no. 1, pp. 251–262, Mar. 2022.

[11] W. Zhu, C. Chen and S. Duan, "Model predictive control with improved discrete space vector modulation for three-level Vienna rectifier," IET Power Electron., vol. 12, no. 8, pp. 1998–2004, 2019.

[12] B. Xu, K. Liu and X. Ran, "Computationally efficient optimal switching sequence model predictive control for three-phase Vienna rectifier under balanced and unbalanced DC links," IEEE Trans. Power Electron., vol. 36, no. 11, pp. 12268–12280, Nov. 2021.

[13] C. Liu et al., "An improved model predictive control method using optimized voltage vectors for Vienna rectifier with fixed switching frequency," IEEE Trans. Power Electron., vol. 38, no. 1, pp. 358–371, Jan. 2023.

References (2/2)

[14] Z. Gao, "Active disturbance rejection control: A paradigm shift in feedback control system design," in Proc. Amer. Control Conf., Jun. 2006.

[15] R. Zhou and W. Tan, "Analysis and tuning of general linear active disturbance rejection controllers," IEEE Trans. Ind. Electron., vol. 66, no. 7, pp. 5497–5507, Jul. 2019.

[16] J. Li et al., "Passivity-based control with active disturbance rejection control of Vienna rectifier under unbalanced grid conditions," IEEE Access, vol. 8, pp. 76082–76092, 2020.

[17] B. Kedjar, H. Y. Kanaan and K. Al-Haddad, "Vienna rectifier with power quality added function," IEEE Trans. Ind. Electron., vol. 61, no. 8, pp. 3847–3856, Aug. 2014.

[18] H. Ahmed and D. Celik, "Sliding mode based adaptive linear neuron proportional resonant control of Vienna rectifier for performance improvement of electric vehicle charging system," J. Power Sources, vol. 542, Art. no. 231788, 2022.

[19] Y.-H. Liao, B.-R. Xie and J.-S. Liu, "Modeling and control of current sensorless PFC three-phase Vienna rectifier with balanced and unbalanced DC-link voltage," IEEE Trans. Power Electron., vol. 40, no. 3, pp. 4051–4066, 2025.

[20] L. Tian et al., "Voltage sensorless three-phase PWM rectifier control based on linear extended state observer," IEEE J. Emerg. Sel. Topics Power Electron., vol. 13, no. 5, pp. 6562–6574, 2025.

[21] Y.-H. Liao, W.-H. Hsu and B.-R. Xie, "A linearized time-invariant voltage-sensorless direct power control for three-phase Vienna rectifiers," IEEE Access, vol. 11, pp. 59033–59048, 2023.

[22] H.-C. Chen, C.-Y. Lu and G.-T. Li, "Design and implementation of three-phase current sensorless control for PFC bridge converter with considering voltage drops of power semiconductors," IEEE Trans. Ind. Electron., vol. 65, no. 12, pp. 9234–9242, 2018.

[23] S. Bayhan and H. Komurcugil, "A current sensorless control method for multi-level active front-end rectifiers with LCL filter," IET Power Electron., vol. 16, no. 5, pp. 715–727, 2023.

[24] N. N. Nam et al., "Voltage sensorless model predictive control for a grid-connected inverter with LCL filter," IEEE Trans. Ind. Electron., vol. 69, no. 1, pp. 740–751, Jan. 2022.

[25] B. Xu, K. Liu, X. Ran, Q. Huai and S. Yang, "Model predictive duty cycle control for three-phase Vienna rectifiers with reduced neutral-point voltage ripple under unbalanced DC links," IEEE J. Emerg. Sel. Topics Power Electron., vol. 10, no. 5, pp. 5578–5590, Oct. 2022.

[26] S. Xie, Y. Sun, M. Su, J. Lin and Q. Guang, "Optimal switching sequence model predictive control for three-phase Vienna rectifiers," IET Electr. Power Appl., vol. 12, no. 7, pp. 1006–1013, 2018.

Thank You!

Upcoming Programmes

Engineering College of Technology (ECT) *UK-Recognised Qualifications*	Start Date
Bachelor of Engineering (Honours) in Industrial Automation	February 2027
Bachelor of Engineering (Honours) in Electrical Engineering	February 2027
Master of Science (Power System Analysis and Renewable Integration)	February 2027
Master of Science (Industrial Automation and Instrumentation Control)	February 2027

Professional Certificates

Looking to upskill further? Check out the Professional Certificates!

These **3-month, non-accredited Professional Certificates of Competency**, delivered by ECT's affiliated institute, EIT, are designed by industry leaders and academics for technicians, technologists, engineers, and engineering professionals seeking to advance their expertise in a specific area. Featuring live, interactive webinars led by expert instructors with technical know-how, along with dedicated learning support, these courses are the perfect complement to an existing degree, qualification, or relevant work experience.

Find out more!

Contact Us:

Website
www.ect.ac.uk

Programmes
https://www.ect.ac.uk/programmes/

Head Office
Whittle Way, Stevenage SG1 2FS,
United Kingdom

Phone
Inside UK: 0203 582 1389
Outside UK: +44 203 582 1389

UKPRN: 10089771